Transactions of the Materials Research Society of Japan 33[2] 385-388 (2008)

Nucleation of Cubic Phase in Deeply Undercooled Melt of Anisotropic Material

Kiyoshi Nozaki*, Kosuke Nagashio and Kazuhiko Kuribayashi
Institute of Space and Astronautical Science (ISAS), Japan Aerospace Exploration Agency (JAXA)
3-1-1 Yoshinodai, Sagamihara, Kanagawa 229-8510, Japan
*Corresponding author: kiyoshi.nozaki@isas.jaxa.jp

α-$FeSi_2$ alloys were solidified from undercooled melts on electromagnetic levitator. The in-situ observation of the solidification behavior was conducted using a high-speed video recorder. At ΔT >100 K, the sword-like dendrite with hexagonal symmetry was shown, despite the tetragonal structure of α-$FeSi_2$. In this study, the formation of six-fold dendrite from undercooled melts was examined from the point of view of the competitive nucleation based on the analysis of crystallographic orientation using an electron backscattering pattern apparatus. We propose that the six-fold symmetry resulted from the three different crystals growing into the <110> direction of the (111) plane of the metastable cubic phase of γ-$FeSi_2$.

Key words: crystal growth; crystal structure; anisotropy

1. INTRODUCTION

An electromagnetic levitation (EML) has been applied to reveal the solidification behavior of electronic conductor from undercooled melts as a function of undercoolings because they can remove the crucible wall which is the preferential site of heterogeneous nucleation. During solidification into undercooled melts, the negative temperature gradient built ahead of the solid-liquid interface destabilizes the interface morphology to a dendritic one. For simple metals, dendrites preferentially grow into the direction of the minimum surface stiffness. On the other hand, monatomic semiconductors with a diamond structure show the substantial change of macroscopic growth interface as a function of undercoolings [3,4], because it has stronger anisotropy than simple structures of metals. Recently, authors reported [5] an *in-situ* observation of containerless solidification in the anisotropic α-$FeSi_2$ with c/a=1.91 [6]. The growth morphology drastically changed depending on the undercooling, ΔT. The faceted planes were observed on the surface of the sample at ΔT <~50 K. With increasing undercoolings, the morphology changed into typical facet dendrite. Especially at the high undercooling of ΔT >~100 K, a dendrite with the hexagonal symmetry clearly appeared. The growth velocities were measured as a function of undercooling and compared with the classical dendritic growth theory [7]. The kinetics coefficient of α-$FeSi_2$ was calculated to be much smaller than those of typical metallic and semiconductor materials with simpler crystal structures. This result indicates that the interfacial kinetics is dominant in the growth of α-$FeSi_2$.

In the present study, we employed the rapid quenching of the sample and subsequent observation microstructures were conducted based on the previous results, to focus on the growth mechanism behind the six-fold symmetry. Then, the growth kinetics was discussed in relation with the anisotropy of crystal structure in order to give some suggestions on the solidification mechanism of other intermetallic compounds.

2. EXPERIMENTAL

The alloy was arc-melted from Fe of 99.9% purity and Si of semiconductor grade. The ingot was cut into small pieces of ~0.6 g. An electromagnetic levitation (EML) chamber was initially evacuated to 10^{-4} Pa by a turbo molecular pump and then backfilled with argon gas to a positive pressure [5]. The sample, which was levitated and heated to the temperature 100 K higher than the melting point, was cooled by blowing helium gas of 99.999 % purity. At a specified undercooling, the melt was triggered to nucleate with an alumina needle. Temperatures of samples were monitored by a two-color pyrometer, the wavelengths of which were 900 and 1550 nm. The measurement error of the pyrometer was less than 0.5% of the full range. A high-speed video recorder (HSV) with spatial resolution of 400×280 pixels was operated at 2 kHz to monitor the morphology and the velocity of growing crystals during recalescence. In addition, the droplet held at temperatures approximately the

melting point (T_M=1493K) was fallen onto a silicon chill plate to quench the microstructure formed at the early stage of the solidification. The microstructure of the quenched surface was examined using an optical microscope and a scanning electron microscope (SEM). The crystallographic texture was also examined using the electron backscattering pattern (EBSP) apparatus (Tex-SEM Laboratories, Inc.).

3. RESULTS

Figure 1 shows typical snapshots taken by the HSV recorder during recalescence and the optical micrograph of as-solidified sample at ΔT = 100 K. As shown in Figure 1(a), the dendrite morphology was a six-fold symmetry like a snow-crystal, as if the sword-like dendrite had grown radially from the nucleation point and shaped a pattern of a six-fold symmetry. However, it was difficult to find the hexagonal symmetric dendrites on the surface of the as-solidified sample shown in Figure 1(b) because they had been covered with the solidification of the remaining melts after recalescence [3]. Therefore, we conducted splat quenching of the droplet onto a silicon wafer to freeze the hexagonal dendritic microstructure in Figures 2. The morphology and size of the crystal are similar to those of the dendrite shown in Figure 1(a), which implies that the dendrite

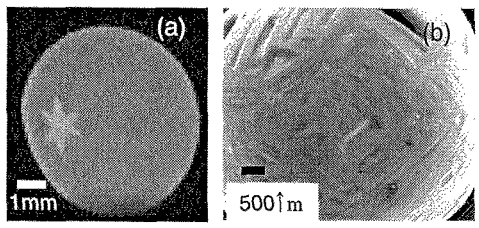

Fig. 1 (a) Solidification behavior of α-$FeSi_2$ observed by the HSV at 100 K. (b) SEM image of surface morphology of the as-solidified sample at ΔT= 100 K. The facet plane was not found on the surface..

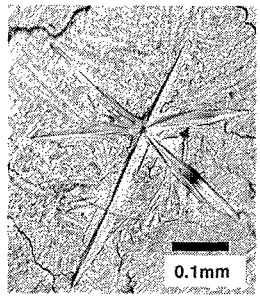

Fig.2 The image of an optical micrograph of the splat-quenched sample. The hexagonal dendrite is clearly seen.

with six-fold symmetry that appears at the early stage of the recalescence in the deeply undercooled melt was frozen on the quenched surface. Figure 3 shows the corresponding EBSP map of the quenched surface of the sample. The EBSP map shown in 3, where the color was referred on the normal direction, clearly indicates that all facetted crystals developed on the {112} plane. Figure 4 indicates the growth direction of the variant, which was fixed to the rolling direction, is <110> direction. This result of EBSP maps indicates that the crystal with six-fold symmetry consists of three different variants oriented as [110]{100}.

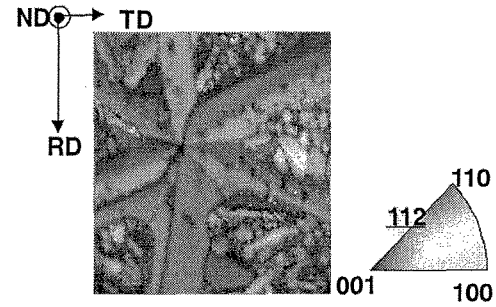

Fig. 3 EBSP mapping of the ND direction of the splat-quenched sample. The hexagonal dendrite lies on the {112} plane.

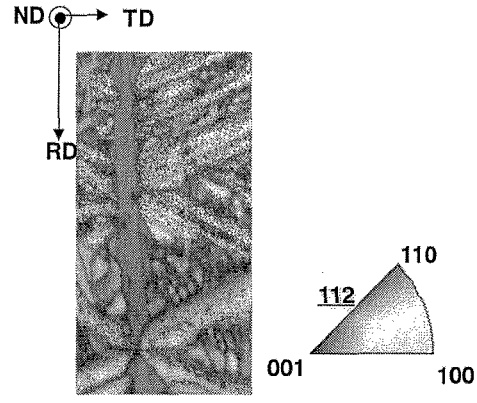

Fig. 4 The EBSP mappings of the RD direction of the splat-quenched sample. The hexagonal dendrite consists of three single crystals; the directions of all arms of the hexagonal dendrite are <110>.

4. Discussion

We discuss the hexagonal dendrite growth mechanism of α-$FeSi_2$. Figure 5(a) shows the crystal structure of α-$FeSi_2$. It can be roughly recognized as cubic when four units are placed together, because c/a is close to 2 in spite of tetragonal. The Fe atom in the tetragonal structure exists in only one of two cubic units. From the

results of EBSP, the hexagonal dendrite, which is oriented to the [110] {112} plane, consists of three different variants. Three sides on the {112} plane, however, are not crystallographically equivalent; only one direction is <110> and the others are <201>. One hypotheses to resolve this discrepancy is the formation of a facet dendrite growth using twist boundary; two variants share their {112} planes and one crystal unit was rotated by 60 degrees for the other. In this model, two <110> directions can be produced on the shared {112} plane. Similarly, another rotation by 60 degrees provides one more <110> direction. As a result, this twist boundary provides three <110> directions on the {112} plane. This twist boundary model, however, does not provide crystallographic grounds for the well-regulated angular relationship of the boundary on the {112} plane. In fact, the twist boundary of α-$FeSi_2$ with a 60-degree rotation is a Σ3 boundary, but not a twin boundary because {112} is not the mirror plane. Considering the number of atoms per unit area, {112} is not the most densely packed plane in α-$FeSi_2$. Additionally, in order that the {112} plane is to be a twist boundary plane, approximately half the number of the Fe atoms has to be removed and the Si atoms are shuffled to the symmetrical sites on the {112} plane, which may largely distort the crystal lattice. The constant appearance of the six-fold dendrite requires a mechanism to maintain the angular relationship between the unit cells.

Here, we noticed the cubic structure of γ-$FeSi_2$ (Figure 4(b)), which is a metastable phase of $FeSi_2$. The formation of γ-$FeSi_2$ was confirmed in the epitaxial crystal of Fe-implanted Si (001) substrate. γ-$FeSi_2$ exists between Si substrate and α-$FeSi_2$ to relax the lattice mismatch in the interface [9]. The plane {112} of tetragonal α-$FeSi_2$ is equivalent to the plane {111} of cubic γ-$FeSi_2$, which has three identical <110> directions. When α-$FeSi_2$ starts growing in the <110> directions from the {111} plane of γ-$FeSi_2$, the six-fold dendrite can be formed without a 60-degree rotation on the {112} plane of α-$FeSi_2$. In our experiment, although γ-$FeSi_2$ was undetectable even in the quenched samples, the shape of the crystal with six-fold symmetry strongly suggests that the initial phase formed in deeply undercooled melts is to be a phase with a cubic lattice. Authors, on the basis of the neg-entropy model for solid-liquid interfacial energy, have proposed a model for phase selection between stable and metastable phases during the solidification into undercooled melt [9]. This model shows that the critical factor in the phase selection is the ratio of the entropy of fusion of a metastable phase to that of a stable phase: the smaller entropy of fusion facilitates the metastable phase to be nucleated more frequently even at a lower undercooling. Figure 6 shows the schematic drawings of the Gibbs free energies as a function of temperature for phases, melt (P_m), stable phase (P_s) and metastable phase (P_{ms}). The slope of G(T) corresponds to the negative entropy. The relationship $S_m > S_{ms} > S_s$ commonly exists in these states. Thus, it can be understood that the fusion entropy of metastable phase, ΔS_{ms}, is smaller than that of stable phase, ΔS_s. The high entropy phase such as cubic γ-$FeSi_2$ can be nucleated when the undercooling is larger than the critical one. The existence

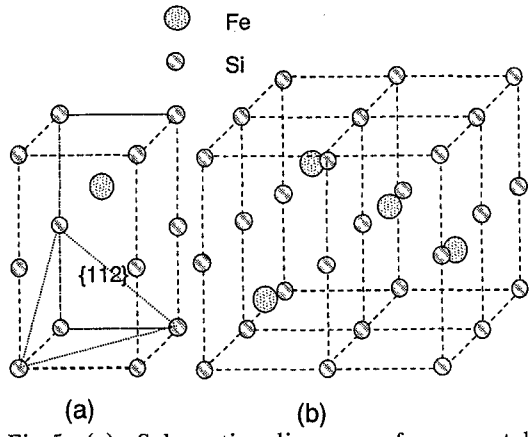

Fig.5 (a) Schematic diagram of a crystal structure of α-$FeSi_2$. (b) Schematic diagram of a crystal structure of γ-$FeSi_2$. It is noted that this schematic is re-drawn using Si frame in order to compare it easily with (a).

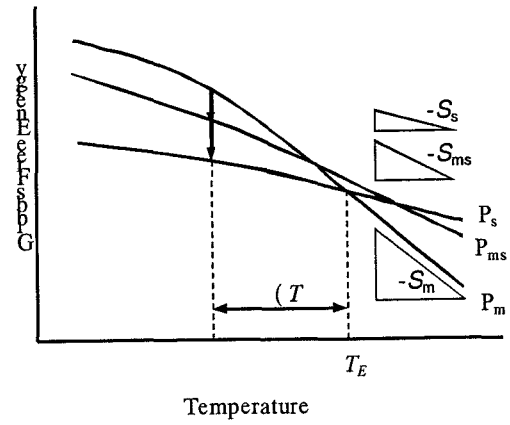

Fig.6 Schematic presentation of the temperature dependence of the Gibbs free energies for phases, melt (P_m), stable phase (P_s) and metastable phase (P_{ms}), showing the relation, $\Delta S_s > \Delta S_{ms}$.

of this cubic phase, γ-$FeSi_2$, is thermodynamically appropriate because it shows a strong tendency to develop a cubic phase or a phase with high symmetry just below the melting temperature, in addition to reporting the existence of γ-$FeSi_2$ [8].

V Conclusions

In-situ observation of α-$FeSi_2$ and microstructure analysis elucidated the growth mechanism of α-$FeSi_2$ as a function of undercoolings. EBSP analysis on the hexagonal facet dendrites indicated that the six-fold symmetry resulted from the three different crystals of α-$FeSi_2$ growing in the <110> direction. Based on the crystallographic and thermodynamic considerations, we proposed that the cubic γ-$FeSi_2$, which is a disorder phase of α-$FeSi_2$, was formed first and then hexagonal facet dendrites of α-$FeSi_2$ began to grow in the <110> directions from the {111} plane of γ-$FeSi_2$.

Acknowledgements

This study was financially supported by a Grant-in-Aid for Scientific Research from the Ministry of Education, Culture, Sports, Science and Technology, Japan.

[1] D. Li, K. Eckler, D.M. Herlach, J.Cryst. Growth 160 (1996) 59.
[2] Y. Saito : *Statistical Physics of Crystal Growth* (World Scientific Publishing, Singapore, 1996) pp. 86-87.
[3] T. Aoyama, Y. Takamura, K. Kuribayashi, Metall. Mater. Trans. A 30A (1999)1333.
[4] T. Aoyama, K. Kuribayashi, Acta Mater. 48 (2000) 3739.
[5] K. Nozaki, K. Nagashio and K. Kuribayashi: Metall. Mater. Trans. A (in press).
[6] F.A. Sidorenko, P.V. Gel'd, L.B. Dubrovskaya, Fiz.Met.Metalloved. 8 (1959) 735.
[7] J. Lipton , W. Kurz and R. Trivedi: *Acta. Metall.*, 35(1987) 957.
[8] M. Behar, H. Bernas, J. Desimoni, XW. Lin XW and R.L.Maltez: *J. Appl. Phys.*, 79(1996) 752.
[9] K. Kuribayashi, K. Nagashio, K. Niwata, M. S. Vijaya Kumar and T. Hibiya; *Mat. Sci. Eng A,* 449-451(2007) 675.

(Recieved October 22, 2007 ; Accepted November 9, 2007)